# Domain walls unmasked during domain duplication in ferromagnetic tunnel junctions

P. Rottländer, M. Hehn, F. Elhoussine, O. Lenoble, and A. Schuhl
*Laboratoire de Physique des Matériaux, UMR CNRS 7556, Boîte Postale 239, 54506 Vandoeuvre lès Nancy Cedex, France*
(Received 1 July 2003; published 27 February 2004)

This paper highlights the role played by domain walls during domain duplication in ferromagnetic junctions. The evolution of the resistance jumps with reversal field when duplication occurs cannot be exclusively explained by parallel tunnel paths of electrons through regions with parallel and antiparallel magnetization alignment. A model of tunnel resistance taking into account the contribution of domain walls was used to extract their density. The extracted values are in agreement with experimental data.

DOI: 10.1103/PhysRevB.69.064430 PACS number(s): 75.60.−d, 73.40.Rw, 75.40.Mg, 75.47.De

## I. INTRODUCTION

Spin electronic devices require the understanding and the control of the magnetic properties of their ferromagnetic (FM) electrodes. Often in such devices, two magnetic electrodes are separated by a thin layer, an insulator for magnetic tunnel junctions (MTJ's), and an important parameter is the coupling between the two electrodes of the MTJ. Indeed, these interactions influence the reversal characteristics of the FM layers, and thus, the magnetoresistive response of the tunnel device. Magnetic couplings between two FM films separated by a thin insulating layer can originate from several mechanisms.[1–4] However, considering continuous and pinhole-free insulating layers and negligible voltage dependent coupling,[1] the most important class of interactions are magnetostatic. In this last category, two main contributions have been identified. The first one is the antiferromagnetic coupling related to the lateral flux closure of the stray fields between the magnetic layers of the MTJ. It becomes significant when reducing the lateral size of the MTJ FM electrodes and increasing their aspect ratio.[2] The second contribution is related to stray fields induced by magnetic charge accumulations in the junction's ferromagnetic layers and are usually associated with the roughness of the interfaces, referred to as the orange-peel effect.[3,4]

It has been found that if the two magnetic layers in contact with the insulating barrier are coupled ferromagnetically via the orange-peel effect,[5] a duplication of the domain structure in the soft layer from the hard magnetic layer template can occur.[6] In fact, the stray field of each domain of the hard magnetic layer can locally either increase or decrease the magnetic field seen by the soft layer, depending on the orientation of their magnetizations with respect to the applied field. So, this nonhomogeneous field can sequentially reverse parts of the soft layer and so induce a domain structure in the soft layer. When domains are duplicated, the tunnel junction appears to be in a fully parallel state from a tunnel magnetoresistance (TMR) signal point of view, even if domains with opposed magnetizations remain in each layer.

Nevertheless, up to now, the contribution of the domain walls to the electrical resistance of the tunnel junction has been neglected. Their presence has however been shown to play an important role in the TMR signal[7] and this has been used to study their stability.[8]

After a brief description of the sample structure and fabrication, we show that the junctions under consideration present the domain duplication phenomena. Then, the evolution of the resistance jumps when duplication occurs cannot be exclusively explained by parallel tunnel paths of electrons. Taking into account domain walls allows one to find the origin of this discrepancy and also to extract the field dependent wall density.

## II. SAMPLES FABRICATION

Junctions are deposited onto float-glass substrates using a sputtering system with cobalt (Co) and aluminum (Al) targets mounted on dc magnetron cathodes, and iron (Fe), permalloy (Py), and tantalum (Ta) targets mounted on rf magnetron cathodes. Details on the junction fabrication (oxidation process to make the alumina tunnel barrier in the following, denoted $AlO_x$) and on the experimental setup used to characterize the junctions can be found elsewhere.[5] The structure of the samples under study is glass/Ta (10 nm)/$Co_{80}Fe_{20}$ (8 nm)/Co (2 nm)/$AlO_x$ (1.35 nm, oxidation time $y$ s)/Py (20 nm)/Ta (10 nm) where the thickness of each layer is given in the brackets in nanometers. Deposition conditions of the soft Py (20 nm) and of the hard $Co_{80}Fe_{20}$ (8 nm)/Co(2 nm) have been optimized such that the easy axis of both layers are parallel and that magnetization reversal in both cases occurs by nucleation and propagation of domain walls. The aluminum layer oxidation time $y$ has been optimized to get the maximum TMR signal. The processed junctions show the typical nonlinear $I$-$V$ curve and an increase of conductivity with increasing temperature, which is generally seen as a sign of the absence of pinholes.[9]

## III. DOMAIN DUPLICATION AND TMR CYCLE

Complete (−) and minor characteristic TMR cycles measured on an oxidation optimized tunnel junction with $AlO_x$ (1.35 nm, oxidation time 30 s) are shown in Fig. 1. In this sample, the strength of the dipolar coupling between the electrodes has been determined to be $H_d = 6$ Oe, from the shift of the minor TMR cycle in which only the soft layer is switched (not shown). This value is two times lower than previously reported values with the same barrier but other magnetic electrodes.[5] Nevertheless, this value is strong enough to ensure domain duplication and extend the validity of the observed duplication to new couples of magnetic ma-

 

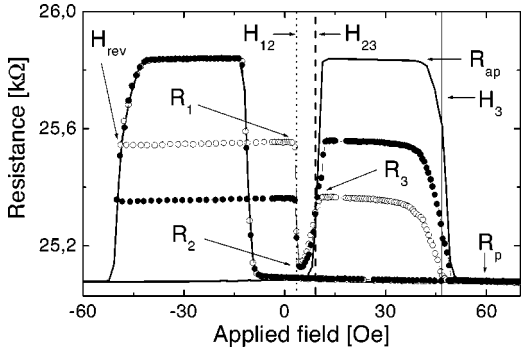


FIG. 1. Complete (−) and minor tunnel magnetoresistance loops measured on a glass/Ta (10 nm) $Co_{80}Fe_{20}$ (8 nm)/Co(2 nm)/$AlO_x$ (1.35 nm, oxidation time 30 s) Py(20 nm)/Ta(10 nm) tunnel junction made using *ex situ* changed masks with 200 $\mu$m lateral path. The minor cycles have been measured using different $-H_{rev}$ values at which the applied field sequence is reversed : −48.3 Oe (-○-), −49.8 Oe (-●-).

terials. After saturation at +300 Oe, the applied field is decreased down to −300 Oe (complete cycle) or to $-H_{rev}$ (minor cycle). When the step sequence of fields is reversed and the applied field is again positive, the two cycles appear to be completely different.

In the case of the complete negative saturation (complete cycle, continuous line), the cycle is symmetric and therefore holds two resistance jumps. From magneto-optical Kerr effect and AMR (anisotropic magnetoresistance) measurements which were performed separately on each of the magnetic electrodes (Fig. 2) we know that both have a uniaxial

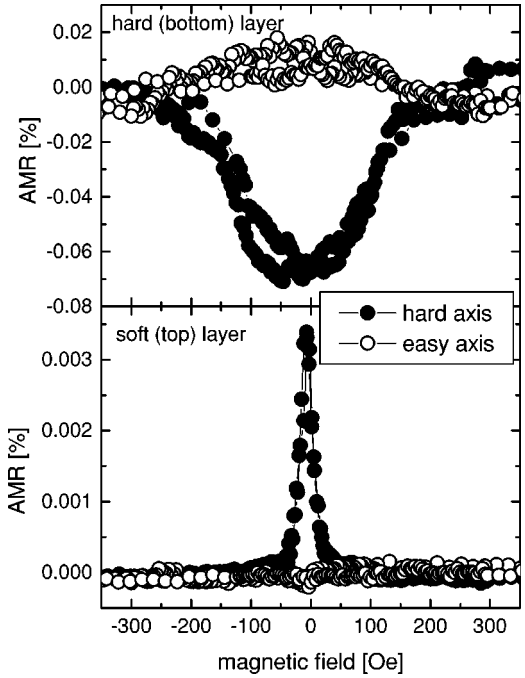


FIG. 2. AMR cycles for the soft and hard electrodes. Both are clearly showing a uniaxial anisotropy. Between the measurements with the field in directions of the hard and easy axes, the sample has been turned by 90° in the magnetic field.

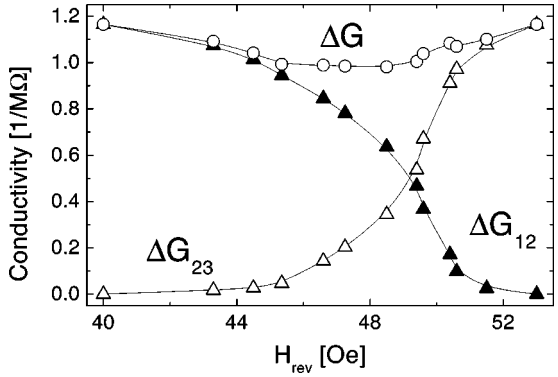


FIG. 3. Variation of the conductance jumps measured for an applied field $H_{12}$ (black triangle) and $H_{23}$ (triangle) as a function of the reversing negative applied field $H_{rev}$. The last curve (○) is a plot of the sum of the conductance jump absolute values measured at $H_{12}$ and $H_{23}$. The lines are guides for the eyes.

anisotropy. Any deviation from antiparallel alignment therefore should result in a considerably rounded curve in the high-resistance state. From the clear plateau of constant high resistance we therefore conclude that we achieve a fully antiparallel state.

The transition between low and high resistance is confined to a small field range, but within this range it appears smooth. As we know from the very existence of the domain duplicated state that the hard magnetic layer reverses its magnetization by movement of domain walls, conduction through ballistic pinholes or a small area of the junction should lead to a noncontinuous magnetoresistance curve. We therefore can exclude effects which could arise from a nonhomogeneous magnetoresistance effect. These are the reasons why we chose the present samples for further investigation. It will be shown later that any nonpolarized excess current—which might be due to leakages or barrier defects—in fact does not influence the results. Those junctions appear as well-suited model systems to study the domain duplication phenomena.

In the case of minor cycles, three resistance jumps with different signs appear at fields named $H_{12}$, $H_{23}$, and $H_3$ along the (0, +300 Oe) field branch and the cycle is asymmetric.

In order to get a much simplified discussion, we now have to switch from the more familiar resistances to conductances; we define $G_1=1/R_1$, $G_2=1/R_2$, $G_3=1/R_3$. The variation of the conductance jump amplitudes for the previously defined applied fields $H_{12}$, $\Delta G_{12}=G_2-G_1$, and $H_{23}$, $\Delta G_{23}=G_2-G_3$, are reported in Fig. 3. The last curve added to the plot is the sum of these two conductance jumps,

$$\Delta G=\Delta G_{12}+\Delta G_{23}. \tag{1}$$

For applied fields between $H_{12}$ and $H_{23}$ in Fig. 1, the junction resistance is close to the one measured when the magnetizations of the two magnetic electrodes are in a parallel configuration. Therefore, directly across the barrier, the magnetizations of the two magnetic electrodes are locally parallel even if the hard magnetic layer is far from magnetic saturation.[6] As a consequence, the domain structure of the

hard layer is duplicated in the soft layer. A detailed analysis of the duplication process can be found elsewhere.[5] Depending upon the choice of $-H_{rev}$ around the field needed to reverse the hard $Co_{80}Fe_{20}$ (8 nm)/Co(2 nm) bilayer, the relative amount of reversed and nonreversed domains is being established in the hard layer and it changes the relative amplitude of the conductance jumps measured at $H_{12}$ and $H_{23}$.

## IV. EFFECT OF DOMAIN WALLS ON THE JUNCTION RESISTANCE

### A. Contribution from the domains

As $-H_{rev}$ decreases towards negative fields, $\Delta G_{12}$ decreases while $\Delta G_{23}$ increases as shown in Fig. 3. This trend can be understood considering that electrons tunnel through the barrier using the shortest path, i.e., perpendicular to the metal/insulator interface. Then, the existence of reversed domains in the hard layer creates locally high conductance tunneling paths which augment the overall conductance on the $(-H_{rev},0)$ branch, compared to a fully antiparallel configuration. Indeed, the conductance of the junction can be seen as resistors in parallel whose values depend on the orientation of the magnetizations each apart the junction. To take into account possible leakage currents, we will use the intrinsic conductivities in the parallel and antiparallel alignment, $\gamma_p$ and $\gamma_{ap}$, and an overall nonpolarized leakage conductivity $G_l$ (which might or might not be homogeneously distributed over the junction). The measured conductances in parallel and antiparallel alignment can thus be expressed as

$$G_p = S\gamma_p + G_l, \tag{2}$$

$$G_{ap} = S\gamma_{ap} + G_l, \tag{3}$$

$S$ being the total junction area. Similarly, the conductances of the junction before, during, and after duplication (Fig. 4) are equal to

$$G_1 = S_{nr}\gamma_{ap} + S_r\gamma_p + G_l, \tag{4}$$

$$G_2 = S\gamma_p + G_l, \tag{5}$$

$$G_3 = S_{nr}\gamma_p + S_r\gamma_{ap} + G_l, \tag{6}$$

where $S_{nr}$ ($S_r$) is the total surface of the domains with magnetization oriented along (opposite) the positive saturation field.

Decreasing $-H_{rev}$ decreases the value of $S_{nr}$ and so $\Delta G_{12}$. In contrast to our previous work,[5] it appears that $\Delta G$ is not constant in the field window where duplication occurs but has a parabolic variation with a minimum value for $-H_{rev}$ around the coercive field of the hard magnetic layer (Fig. 3). This statement is of particular importance since it will unmask the domain walls using their contribution to the resistance of the junction.

From Eqs. (4)–(6), and using the definition of $\Delta G$ in Eq. (1), we find

$$\Delta G = S(\gamma_p - \gamma_{ap}), \tag{7}$$

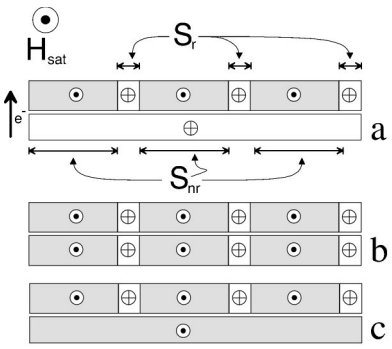


FIG. 4. Sketch showing the evolution of the domain structure in the hard $Co_{80}Fe_{20}$ (8 nm)/Co (2 nm) bilayer (top layer) and the soft Py (20 nm) layer (bottom layer) for an increasing applied field: (a) before, (b) during, and (c) after domain duplication. The symbols ⊙ and ⊗ represent the main magnetization in each domain (oriented perpendicular to the paper sheet), respectively, opposite and along the positive saturating field (represented by the big ⊙ outside the sketch). The arrow, outside the drawings perpendicular to the two magnetic layers, exemplifies the electron trajectory through the tunnel junction. After a positive saturation, the applied field is decreased and reversed until $-H_{rev}$ is reached. At this field, the soft Py layer is saturated negatively and a domain structure remains in the hard $Co_{80}Fe_{20}$ (8 nm)/Co(2 nm) bilayer [sketch (a)]. The total surface of the domains oriented along (inverse) the positive saturating field is $S_{nr}$ ($S_r$). As the magnetic field $H$ is reversed from $-H_{rev}$ towards the positive fields, regions of the soft layer which are located over domains in the hard layer with main magnetization oriented in the positive field direction experience a local field equal to $H+H_d$. Therefore, these regions will rotate first [sketch (b)]. A further increase of $H$ leads to the reversal of regions of the soft layer which are located over domains in the hard layer with main magnetization oriented in the negative field direction and experience a local field equal to $H-H_f$. These regions will then switch in a second step [sketch (c)].

which is the conductance change between parallel and antiparallel alignment. This value is independent of the reversing field $-H_{rev}$, or a leakage current. The observed dependence of $\Delta G$ on $-H_{rev}$ thus cannot be explained within this model.

### B. Contribution from the domain walls

It appears from a close examination of Fig. 1 that, in the field window for which duplication occurs, the resistance of the junction never reaches the one measured for the parallel alignment of the electrode magnetizations. Furthermore, the value of conductance $G_2$ varies with $-H_{rev}$.

Since the change of $G_1+G_3$ does not exceed 0.03 $M\Omega^{-1}$, the main variation of $\Delta G$ with $H_{rev}$ arises from the one of $2G_2$. The junction presents the conductance $G_2$ in the duplicated state [Fig. 5(a)]. The only way to explain such a large change of $G_2$ is to take into account the conductance of the domain walls and that their area density evolves with $H_{rev}$.

In this case in the duplicated state, the existence of domain walls in the two magnetic layers creates locally low-conductance tunneling paths due to their local nonparallel alignment which decrease the total tunnel current. The con-

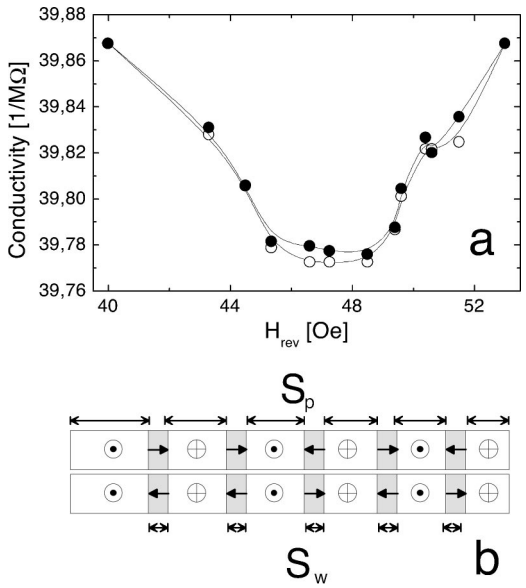


FIG. 5. (a) Variation of $\Delta C_2$ (-○-) and $(\Delta C+C_p+C_{ap})/2$ (-●-) with $H_{rev}$. The lines are guides for the eyes. (b) Sketch showing the domain structure in the two magnetic layers when duplication occurs. From one side to the other side of the barrier, magnetizations in the domains are parallel. The domain walls act as parallel paths and have to be considered in the expression of the junction resistance. Energy considerations make the antiparallel alignment of the wall core magnetizations favorable. The total surface of the walls (domains) is $S_w$ ($S_p$).

ductance of the junction can then be modeled by a network of resistors in parallel associated to domains with magnetizations aligned parallel and domain walls. Again we shall take into account the effect of any possible unpolarized leakage conductance $G_l$ which might be localized or not. $G_2$ can be expressed by

$$G_2=S_p\gamma_p+S_w\gamma_w+G_l, \tag{8}$$

where $S_p$ ($S_w$) is the surface of domains (domains walls) and $\gamma_w$ is the intrinsic conductivity of the walls, with $\gamma_p>\gamma_w>\gamma_{ap}$.

It was established[10] that the particular features of Néel walls, namely, a narrow core region bounded by extremely extended tails are due to the existence of strong volumic dipolar charges. If two layers bearing symmetrical Néel walls are separated by a thin spacer, antiferromagnetic coupling of their core magnetizations will strongly decrease their energy by flux closure of the magnetic stray field. This deeply modifies the wall profiles leading to shorter wall tails and larger core region.[10] In the light of those considerations and as the first approximation, we can consider that the core magnetizations of the domain walls are antiparallel aligned [Fig. 5(b)] and that their conductance $\gamma_w$ is equal to $\gamma_{ap}$. Combining Eqs. (2), (3), and (8), we obtain

$$G_2=\frac{S_p}{S}G_p+\frac{S_w}{S}G_{ap}. \tag{9}$$

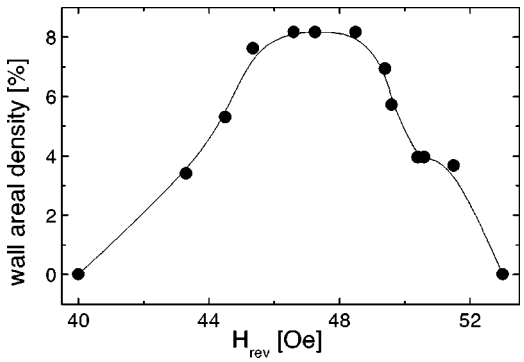


FIG. 6. Evolution of the exacted wall area density as a function of $H_{rev}$. The lines are guides for the eyes. The wall density is the highest for $H_{rev}$ values around the coercive field of the magnetic hard $Co_{80}Fe_{20}$ (8 nm)/Co(2 nm) bilayer.

We see that the leakage conductivity does not appear any more in the equation. As a consequence, the domain area density can be extracted as function of $H_{rev}$ (and turning again to the more familiar resistances),

$$\Delta_w=\frac{S_w}{S}=\left(\frac{1}{R_p}-\frac{1}{R_2}\right)\left(\frac{1}{R_p}-\frac{1}{R_{ap}}\right)^{-1}. \tag{10}$$

Here it should be noted that $\Delta_w$ is independent of a possible presence of any sort of leakage current. Finally, the area density of domain walls $\Delta_w$ varies like $-R_2^{-1}$ and is reported in Fig. 6. This observation could be done owing to the high quality magnetic response achieved for the present tunnel junctions in comparison to $Co/Al_2O_3/Co$ (oxidized) junctions made in a previous work[5] for which those conclusions could not be made. $\Delta_w$ varies like an inverted parabola with the maximum around the coercive field of the hard magnetic layer (Fig. 6). This is in agreement with nucleation and propagation of domain walls during the magnetization reversal in the hard layer: after nucleation, the length of the walls, and so $\Delta_w$, increases until half of the magnetization is reversed. Then, domains contract, and the length of the walls and $\Delta_w$ decrease.

It appears that a maximum of 8% of the junction surface is covered by the walls. This value has been compared to the one extracted from our previous work.[5] In this case, the hard magnetic layer was made with a Co (20 nm) layer which was oxidized after its deposition. The soft magnetic layer was a simple Co layer. From an earlier Kerr microscopy study,[6] a wall area density equal to 2% could be measured considering a wall thickness of 70 nm. Those two values are in reasonable agreement, showing first that 8% is a plausible value for $\Delta_w$ and second that variations of $\Delta_w$ are to be expected when the hard magnetic electrode material is changed.

## V. CONCLUSIONS

In this paper, we highlight the role played by domain walls on the resistance of ferromagnetic tunnel junctions during domain duplication. A brief theoretical description of the process allows us to show that the evolution of the resistance jumps when duplication occurs cannot be exclusively ex-

plained by parallel tunnel path of electrons. A model of tunneling taking into account domain walls was used to extract their density. This work highlights the power of magnetic tunnel junctions to probe the micromagnetic configurations in thin films when the state of one magnetic electrode of the junction is known.

**ACKNOWLEDGMENTS**

The authors thank the company *Alliance Concept* for their technical support and help with the sputtering machine. This work was partly supported by the EC-IST program ''NanoMEM,'' Grant No. IST-1999-13471.

[1] J.C. Slonczewski, Phys. Rev. B **39**, 6995 (1989).
[2] A. Anguelouch, B. Shrang, G. Xiao, Y. Lu, P. Trouilloud, W.J. Gallagher, and S.S.P. Parkin, Appl. Phys. Lett. **76**, 622 (2000).
[3] L. Néel, C.R. Acad. Sci. **255**, 1676 (1962).
[4] S. Demokritov, E. Tsymbal, P. Grünberg, W. Zinn, and I.K. Schuller, Phys. Rev. B **49**, 720 (1994).
[5] M. Hehn, O. Lenoble, D. Lacour, C. Féry, M. Piécuch, C. Tiusan, and K. Ounadjela, Phys. Rev. B **61**, 11 643 (2000).
[6] O. Lenoble, M. Hehn, D. Lacour, A. Schuhl, D. Hrabovsky, J.F. Bobo, B. Diouf, and A.R. Fert, Phys. Rev. B **63**, 052409 (2001).
[7] C. Tiusan, T. Dimopoulos, M. Hehn, V. Da Costa, Y. Henry, H.A.M. van den Berg, and K. Ounadjela, Phys. Rev. B **61**, 580 (2000).
[8] C. Tiusan, T. Dimopoulos, M. Hehn, and K. Ounadjela, Phys. Rev. B **64**, 104423 (2001).
[9] B.J. Jönsson-Åkerman, R. Escudero, C. Leighton, S. Kim, and I.K. Schuller, Appl. Phys. Lett. **77**, 1870 (2000).
[10] J. Miltat, in *Applied Magnetism*, edited by R. Gerber, C.D. Wright, and G. Asti (Kluwer Academic, Dordrecht, 1994), pp. 221–308.